Springer

KSME

Journal of Mechanical Science and Technology 24 (12) (2010) 2577~2585
www.springerlink.com/content/1738-494x
DOI 10.1007/s12206-010-0923-1

Heat transfer characteristics of gaseous slip flow in a micro-channel †

Chungpyo Hong[1,*], Yutaka Asako[2], Koichi Suzuki[1] and Yoon-Eui Nahm[3]

[1]*Department of Mechanical Engineering, Tokyo University of Science, 2641 Yamazaki, Noda, Chiba, 278-8510, Japan*
[2]*Department of Mechanical Engineering, Tokyo Metropolitan University, Minami-Osawa, Hachioji, Tokyo, 192-0397, Japan*
[3]*Department of Mechanical design Engineering, Hanbat National University, Duckmyung-Dong, Yusung-Gu, Daejeon, 305-719, Korea*

(Manuscript Received December 23, 2009; Revised June 16, 2010; Accepted August 6, 2010)

Abstract

Two-dimensional compressible momentum and energy equations with slip boundary conditions are solved to obtain the heat transfer characteristics of gaseous slip flow in a micro-channel with CWT (constant wall temperature) whose temperature is lower or higher than the inlet temperature (cooled case or heated case). The numerical methodology is based on the Arbitrary-Lagrangian-Eulerian (ALE) method. The stagnation temperature is fixed at 300 K and the computations were done for the wall temperature which ranges from 250 K to 350 K. The channel height ranges from 2 to 10 μm and the channel aspect ratio is 200. The stagnation pressure is chosen in such a way that the exit Mach number ranges from 0.1 to 0.7. The outlet pressure is fixed at atmospheric condition. The bulk temperature and the total temperature of the heated case are compared with those of the cooled case and also compared with temperatures of the incompressible flow in a conventional sized channel. Heat transfer characteristics of the gaseous flow are different from those of the liquid flow. And they are also different from each cooled and heated case. A correlation for the prediction of the heat transfer rate of the gaseous slip flow in a micro-channel is proposed.

Keywords: Convective heat transfer; Gaseous slip flow; Micro-channel; Numerical analysis

1. Introduction

Since the experimental work by Wu and Little [1], who measured the heat transfer coefficients for nitrogen flow through micro heat exchanger, numerous experimental and numerical investigations have been undertaken on fluid flow and heat transfer characteristics of micro-channels. Application of a micro-channel to micro-heat exchangers, micro-values, and many other micro-fluidic systems is greatly expected. For instance, one of the applications of a micro-channel with gaseous slip flow is methane reform system for a fuel cell. The system employs many heat exchangers since it includes various chemical processes at various temperatures. The processes are steam reforming, high temperature shift, low temperature shift reaction, and preferential oxidation reaction for the gas purification. The use of a heat exchanger with micro-channels for this kind of the system will reduce the space of the system. Furthermore, a methane reformer which employs micro-channels has been proposed. Ryi et al. [2] have manufactured and tested a micro-channel reformer integrated with a micro-channel combustor. They used methane for reforming process and used air and helium for catalytic combustion.

It is well understood that gaseous flow characteristics in a micro-channel is affected by the combined effect of rarefaction, surface roughness and compressibility. The compressibility effect on the fluid flow characteristics causes the flow to accelerate due to the decrease (variation) of the pressure and density along the channel, which leads to an increase in friction factor. This effect has been addressed by many researchers, e.g. Prud'homme et al. [3], Sun and Faghri [4], Araki et al. [5] and Asako et al. [6, 7]. The rarefaction effect can be studied by solving the momentum and energy equations with slip velocity and temperature jump boundary conditions (e.g. Refs. Arkilic et al. [8], Beskok and Karniadakis [9]). This effect is dominant when the characteristic length of the channel is less than about 10 μm and leads to a reduction in friction factor and heat transfer coefficient with increasing Kn number, as can be seen by Beskok et al. [10], Ahmed and Beskok [11] and Renksizbulut et al. [12]. Recently, Turner et al. [13] conducted experimental investigations to independently show the influence of surface roughness, rarefaction, and compressibility. Hong et al. [14-16] performed numerical investigations to find combined effects of compressibility and rarefaction for a

† This paper was recommended for publication in revised form by Associate Editor Kwang-Hyun Bang

* Corresponding author. Tel.: +81 4 7124 1501(3952), Fax.: +81 7123 9813
E-mail address: hong@rs.noda.tus.ac.jp

wide range of Re and Ma numbers in parallel plate micro-channels and circular micro-tubes. It was found that Poiseuille number (the product of friction factor and Reynolds number, f·Re) is a function of Ma and Kn numbers in the quasi-fully developed region for cases where gaseous flow was accelerated. Also, a number of investigations on heat transfer characteristics of gaseous flow in a parallel plate micro-channel and a circular micro-tube have been conducted. Hadjiconstantinou and Simek [17] studied the influence of rarefaction on the Nusselt number for gas flow between parallel flat plates. Their analysis show a decrease in Nu as Kn increases for both constant wall heat flux and constant wall temperature boundary conditions. Aydin and Avci [18] investigated the effect of viscous dissipation on the heat transfer of incompressible slip flow in micropipes. Turner et al. [19] performed experimental investigation of convective heat transfer for laminar nitrogen gas flow through a micro-channel. They developed the correlation for Ma, Re and Nu to predict the heat transfer. Asako and Hong [20-24] conducted numerical investigations on heat transfer characteristics of gaseous flow in micro-channels and micro-tubes for both cases of constant wall temperature and constant heat flux with no-slip boundary conditions. The discussion above highlights the importance of rarefaction and compressibility effects on the heat transfer characteristics of micro-channels. When the channel size is small and the flow is fast, the heat transfer affected by rarefaction and compressibility effects simultaneously. However, in most of the work, either the rarefaction or compressibility effect has been investigated. There seems to be no parametric study to investigate the simultaneous effects of compressibility and rarefaction on heat transfer of micro-channels. This is a motivation for this study to conduct numerical computations to obtain heat transfer characteristics for gaseous slip flow in a micro-channel whose diameter ranges from 2 to 10 μm.

2. Formulation

2.1 Description of the problem and conservation equations

The problem is modeled as a parallel-plate channel as shown in Fig. 1 with a chamber at the stagnation temperature, T_{stg}, and pressure, p_{stg}, attached to its upstream section. The flow is assumed to be steady, two-dimensional and laminar. The fluid is assumed to be an ideal gas. The governing equations can be expressed as

$$\frac{\partial \rho u}{\partial x}+\frac{\partial \rho v}{\partial y}=0 \tag{1}$$

$$\frac{\partial \rho uu}{\partial x}+\frac{\partial \rho uv}{\partial y}=-\frac{\partial p}{\partial x}+\mu\left(\frac{\partial^2 u}{\partial x^2}+\frac{\partial^2 u}{\partial y^2}\right)+\frac{\mu}{3}\frac{\partial}{\partial x}\left(\frac{\partial u}{\partial x}+\frac{\partial v}{\partial y}\right) \tag{2}$$

$$\frac{\partial \rho uv}{\partial x}+\frac{\partial \rho vv}{\partial y}=-\frac{\partial p}{\partial y}+\mu\left(\frac{\partial^2 v}{\partial x^2}+\frac{\partial^2 v}{\partial y^2}\right)+\frac{\mu}{3}\frac{\partial}{\partial y}\left(\frac{\partial u}{\partial x}+\frac{\partial v}{\partial y}\right) \tag{3}$$

$$\frac{\partial \rho ui}{\partial x}+\frac{\partial \rho vi}{\partial y}=-p\left(\frac{\partial u}{\partial x}+\frac{\partial v}{\partial y}\right)+\lambda\left(\frac{\partial^2 T}{\partial x^2}+\frac{\partial^2 T}{\partial y^2}\right)+\phi \tag{4}$$

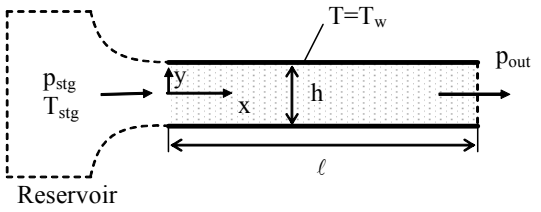

Fig. 1. A schematic diagram of problem.

where

$$\phi=2\mu\left[\left(\frac{\partial u}{\partial x}\right)^2+\left(\frac{\partial v}{\partial y}\right)^2\right]-\frac{2\mu}{3}\left(\frac{\partial u}{\partial x}+\frac{\partial v}{\partial y}\right)^2+\mu\left(\frac{\partial u}{\partial y}+\frac{\partial v}{\partial x}\right)^2 \tag{5}$$

The equation of the state for the ideal gas is expressed by

$$i=\frac{1}{\gamma-1}\frac{p}{\rho}=\frac{R}{\gamma-1}T. \tag{6}$$

For the slip flow (0.001 or 0.01≤Kn≤0.1), it is well known that the rarefaction effect depends on the Knudsen number (Kn= σ /D_h, ratio of the gas mean free path to the characteristic length) and is dominant in which the characteristic length is less than 10 μm under atmospheric pressure and room temperature (Kandlikar and Grande [25]; Karniadakis and Beskok [26]). As mentioned above, such rarefaction effect can be studied by solving the momentum and energy equations with the slip boundary conditions, in which the velocity slip, temperature jump, and shear stress work on the wall are taken into account. Therefore, with the assumptions of slip boundary conditions, uniform inlet velocity, pressure and density and specified pressure, p_{out}, at the outlet are taken as the inlet and outlet boundary conditions. On the wall, thermal boundary condition of constant wall temperature is also considered. Then, the boundary conditions can be expressed as follows:

at the inlet ($x = 0$): $u = u_{in}$, $v = 0$, $p = p_{in}$, $\rho = \rho_{in}$ (7)

at the outlet ($x = \ell$): $p = p_{out}$ (8)

at the walls ($y = \pm 0.5h$): $T = T_w$. (9)

Furthermore, the slip boundary conditions only at the wall are expressed as follows (Sparrow and Lin [27]):
the slip velocity at the wall

$$u_{y=\pm 0.5h}=u_s=\mp\frac{2-F}{F}\sigma\left(\frac{\partial u}{\partial y}\right)_{y=\pm 0.5h},\ v=0 \tag{10}$$

the temperature jump at the wall

$$T_w=T_{y=\pm 0.5h}\pm\frac{2-\alpha}{\alpha}\frac{2\gamma}{\gamma+1}\frac{\sigma}{Pr}\left(\frac{\partial T}{\partial y}\right)_{y=\pm 0.5h}. \tag{11}$$

When there is slip, the shear work due to the slip at wall should be included to calculate the heat flux from the wall. In the previously study [28], the physical reason of the inclusion of the shear work in slip boundary conditions was explained from the point of view of both conservation law of energy and the kinetic theory of gases in detail. Therefore, the shear stress work at the wall

$$\pm\lambda\left(\frac{\partial T}{\partial y}\right)_{y=\pm 0.5h} = \dot{q}_w \mp \mu u_s\left(\frac{\partial u}{\partial y}\right)_{y=\pm 0.5h} \tag{12}$$

where σ is the mean free path, F is Maxwell's reflection coefficient and α is the thermal accommodation coefficient. For fully diffuse reflection, F=1 and if it is assumed that the impinging molecules are accommodated to the wall temperature, α=1 can be used. $\dot{q}_w$ is the heat flux from the wall.

The velocity, the pressure and the density at the inlet of the channel are obtained by the stagnation treatment given by Karki [29]. The stagnation pressure can be expressed in terms of the inlet pressure, velocity and specific internal energy as follows:

$$p_{stg} = p_{in}\left[1+\frac{1}{2}\frac{u_{in}^{\,2}}{\gamma i_{in}}\right]^{\gamma/\gamma-1} \tag{13}$$

Also, from the ideal gas law, the relationship for pressure and density between stagnation and inlet point can be expressed as

$$\frac{p_{stg}}{\rho_{stg}^{\,\gamma}} = \frac{p_{in}}{\rho_{in}^{\,\gamma}} \tag{14}$$

The static pressure at the inlet can be obtained from a linear extrapolation from the interior of the computational domain. By substituting the extrapolated pressure and the stagnation pressure into Eq. (14), the inlet density is obtained. Then, using the equation of state, the specific internal energy at the inlet can be found. Finally, the inlet velocity can be determined by substituting these values into Eq. (13). The procedure is repeated until convergence is achieved.

2.2 Dimensionless variables

Attention will now be focused on the calculation of the Reynolds number, Mach number and Knudsen number that will be defined as

$$\mathrm{Re} = \frac{2\dot{m}}{\mu} = \frac{\bar{u}D_h}{\mu/\bar{\rho}}, \mathrm{Ma} = \frac{\bar{u}}{\sqrt{\gamma(\gamma-1)\bar{i}}}, \mathrm{Kn} = \frac{\sigma}{D_h} = \sqrt{\frac{\pi\gamma}{2}}\frac{\mathrm{Ma}}{\mathrm{Re}} \tag{15}$$

where the $\dot{m}$ is the mass flow rate and D_h is the hydraulic diameter. $\bar{u}$, $\bar{\rho}$ and $\bar{i}$ are the average velocity, density and specific internal energy at a cross-section

$$\bar{u} = \frac{1}{A}\int u\,dA,\ \ \bar{\rho} = \int \rho u dA / \int u dA,$$
$$\bar{p} = \frac{1}{A}\int p\,dA,\ \ \bar{i} = \frac{1}{\gamma-1}\frac{\bar{p}}{\bar{\rho}} \tag{16}$$

The Knudsen number can be used as a measure of the degree of rarefaction of gases encountered in flows through a micro-channel. The Mach number determines the degree of compressibility. As can be seen in Eq. (15), Knudsen number and Mach number are systematically varied to determine their effect on flow and heat characteristics of a micro-channel.

2.3 Numerical solutions

The numerical methodology is based on the Arbitrary-Lagrangian-Eulerian (ALE) method proposed by Amsden et al. [30]. The detailed description of the ALE method is documented in the literature by Amsden et al. [30] and will not be given here. The computational domain is divided into quadrilateral cells. The velocity components are defined at the vertices of the cell and other variables such as pressures, specific internal energy and density are assigned at the cell centers. The cell size 200×20 is chosen, referring our previous study (Hong et al. [14]). The number of cells in the *x*-direction was 200. The cell size gradually increases in x-direction from the inlet to the mid of the channel and it gradually decreases to the exit. The number of cells in y-direction was fixed at 20 for all the computations. The ALE method that is a time marching method is used to obtain the steady solution. The value of 10^{-9} was chosen for the minimum time step. The convergence for time increment was confirmed by inequalities $|\Delta\dot{m}/\dot{m}| < 10^{-10}$, where $\Delta\dot{m}$ represents change in the mass flow rate per every time step. The value of 10^{-3} was used for the convergence criterion of Newton-Raphson iteration in the interior loop of the ALE method.

3. Results and discussion

The computations were performed for three micro-channels of 2, 5, and 10 μm with CWT of T_w=250, 290, 310, and 350 K that is lower or higher than the stagnation temperature, respectively. When air temperature ranges from 250 K to 350 K, C_p, μ and λ of air vary from 1.005 to 1.019 (kJ/(kg·K)), from 1.59×10^{-5} to 2.025×10^{-5} (Pa·s), and from 0.0226 to 0.0293 (W/(m·K)), respectively. The changes in the values are relatively small. Therefore, constant properties are assumed except density. The air of R=287 J·/(kg·K), γ=1.4, $\mu=1.862\times10^{-5}$ Pa·s and λ=0.0261 W/(m·K) was assumed for the working fluid. The channel height ranges from 2 to 10 μm and the aspect ratio of the channel length and height is 200 since developing length for the incompressible flow, ℓ/D_h is 100 at Re=2000. The stagnation temperature was kept at T_{stg}=300 K. The stagnation pressure, p_{stg} was chosen in such a way that the computed Mach number at the exit ranges from 0.1 to 0.7. The outlet pressure was maintained at atmospheric condition, p_{out} =

Table 1. Channel height, ℓ, p_{stg}, Re, Ma, and Kn.

h (μm)	2	5	10
ℓ (mm)	0.4	1	2
p_{stg} (kPa)	400 ~ 1200	300 ~ 800	200 ~ 500
	#1 ~ #5	#6 ~ #9	#10 ~ #13
Re	8 ~ 68	25 ~ 173	37 ~ 253
Ma_{in} Ma_{out}	0.023 ~ 0.065 0.098 ~ 0.697	0.038 ~ 0.101 0.124 ~ 0.744	0.044 ~ 0.119 0.091 ~ 0.597
Kn_{in} Kn_{out}	0.0014 ~ 0.0043 0.0155 ~ 0.0184	8.61×10^{-4} ~ 0.0014 0.0064 ~ 0.0074	6.91×10^{-4}~ 0.0017 0.0035~ 0.0037

10^5 Pa. The channel height, the channel length, the stagnation pressure and the corresponding Re, Ma and Kn numbers for the case of T_w=350 K are listed in Table 1. As the stagnation pressure increases, the corresponding Reynolds number ranges from 8 to 253, and Mach number at the outlet ranges from 0.098 to 0.744. However, the corresponding Knudsen number at the outlet decreases ranging from 0.0035 to 0.0184. Note that the Re is constant along the channel but the Ma varies along the channel. For higher Re the effect of Ma (compressibility) is significant, but for lower Re the Kn effect (rarefaction) is dominant.

3.1 Contour plot of temperature

Contour plots of the temperature for the heated (T_w=350 K) and cooled (T_w=250 K) cases are presented in Figs. 2 and 3, respectively. These are the results for the channel height of h=5 μm. These are typical temperature contour plots for the combination of slow and fast flows in the heated and cooled cases. As can be seen in Figs. 2(a) and 3(a), in the case of the slow flow (Ma_{out} < 0.3), the temperature rises for the heated case and falls for the cooled case very quickly and it becomes almost equal to the wall temperature, respectively. This is similar temperature contour to that of the incompressible flow. On the other hand, in the case of the fast flow (Ma_{out} > 0.3), the temperature fall can be seen near the outlet due to the energy conversion into the kinetic energy caused by the flow acceleration in the core region both heated and cooled cases (Figs. 2(b) and 3(b)). This is the typical temperature contour of the compressible flow. As a result of that, in both heated and cooled cases, the temperature becomes almost equal to the wall temperature when the flow is slow flow, and it falls near the outlet when the flow is fast.

3.2 Heat flux from wall

The heat flux from the wall for both heated and cooled cases in Figs. 2 and 3 is plotted in Fig. 4 along the length. Note that the heat flux has a positive value when $(\partial T/\partial y)_{y=h/2} > 0$. In the case of slow flow represented by the dotted lines, the heat flux from the wall converges to zero asymptotically. This is a

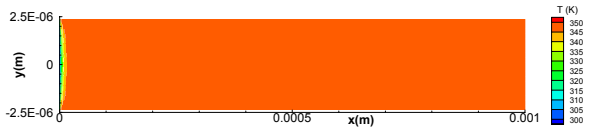

(a) p_{stg}=300 kPa (Ma_{out}=0.124)

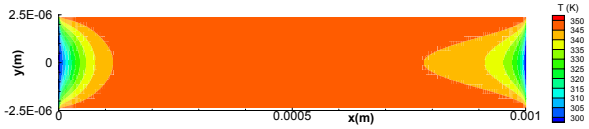

(b) p_{stg}=800 kPa (Ma_{out}=0.744)

Fig. 2. Contour plots of temperature for T_w=350 K.

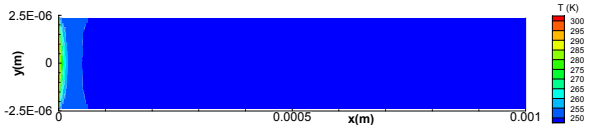

(a) p_{stg}=300 kPa (Ma_{out}=0.143)

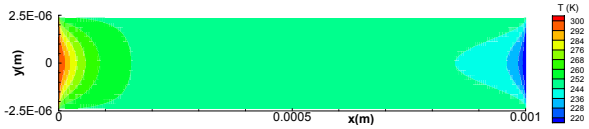

(b) p_{stg}=800 kPa (Ma_{out}=0.812)

Fig. 3. Contour plots of temperature for T_w=250 K.

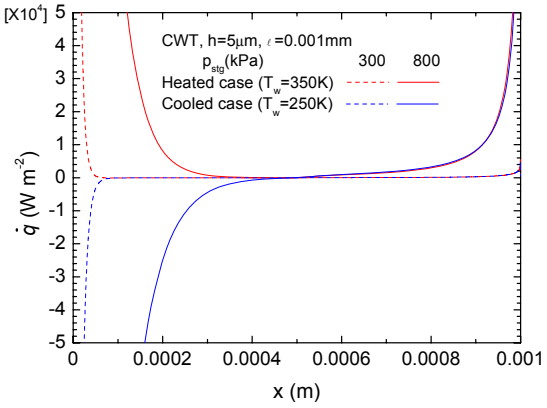

Fig. 4. Heat flux from the wall of h=5 μm.

similar heat flux to that of the incompressible flow. On the other hand, in the case of fast flow represented by the solid lines, part of the thermal energy converts into kinetic energy near the outlet. This results in a temperature drop and additional heat transfer from the wall near the outlet. That is the heat flux increases near the outlet for both heated and cooled cases.

Attention will now be turned to the fast flow of the cooled case, the heat flux has a negative value in the upper half of a channel and has a positive value in the lower half. The reason is that the static gas temperature in the lower half wall becomes lower than the wall temperature due to the energy conversion. Note that the wall plays a cooled role in upper half

and it plays a heated role in lower half of a channel. Therefore the wall for the cooled case takes a different characteristic depending on where flow is slow or fast.

Attention will now be turned to the slip boundary conditions at the wall: slip velocity (Eq. (10)), temperature jump (Eq. (11)) and shear work (Eq. (12)). The value of temperature jump for slow flow (Fig. 2(a)) [illegible] of the heated case is plotted in Fig. 5. [illegible] jump increases along the length and [illegible] ever, the value is less than 0.2 K. Th[illegible] small. The slip velocity defined by Eq. (10) is [illegible]6 along length. In the case of slow flow (p_{stg}=300 kPa), the slip velocity is 4 ms^{-1} and it relatively small. However, in the case of fast flow (p_{stg}=800 kPa), the slip velocity increases along the length and it goes up 30 ms^{-1} steeply at the outlet due to flow acceleration. Then, each term of Eq. (12) is plotted in Figs. 7(a) and (b) for both heated and cooled cases, respectively. The dashed lines represent the left side term of Eq. (12), $\lambda\left(\frac{\partial T}{\partial y}\right)_{y=+0.5h}$, which the heat flux from the wall obtained between the temperature at y=0.5 [illegible] gas temperature adjacent to the wall. The dotted lines represent the seco[illegible] of Eq. (12), $-0.5\mu u_s\left(\frac{\partial u}{\partial y}\right)_{y=+0.5h}$, whic[illegible] shear stress work worked by slip vel[illegible]l. Then, it takes a positive and increase along the channel as the flow accelerates for both heated and cooled cases. As a result of that, the heat flux from the wall, $\dot{q}_w$, for slip flow regime represented by solid line has positive value after the entrance region and increases along the channel. In the heated case (see Fig. 7(a)), $\dot{q}_w$ is slightly lower than $-\mu u_s\left(\frac{\partial u}{\partial y}\right)_{y=+0.5h}$ since $\lambda\left(\frac{\partial T}{\partial y}\right)_{y=+0.5h}$ has a negative value in the range from x=0.00025 to x=0.0005 due to viscous dissipation.

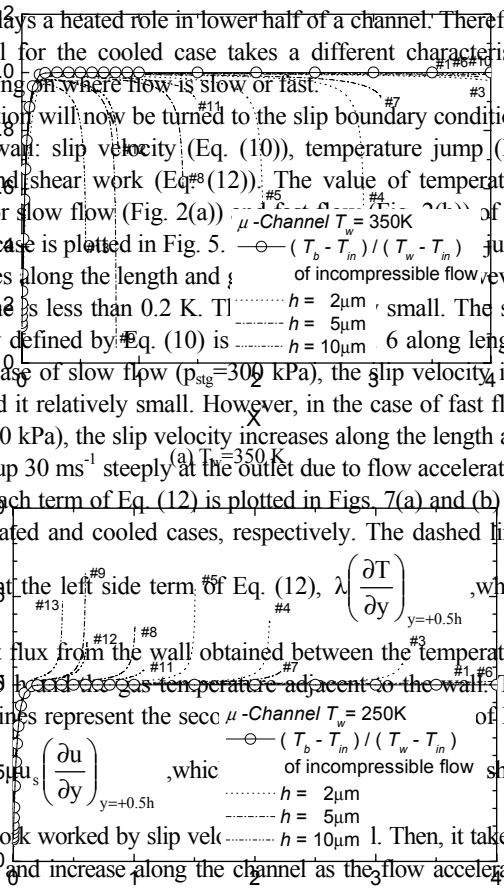

Fig. 8. Bulk temperature as a function of X*.

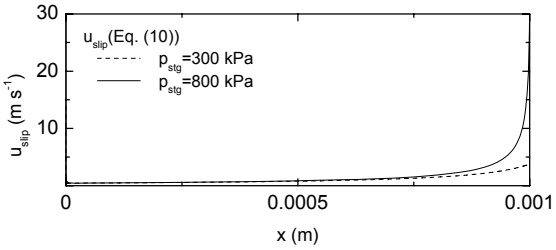

Fig. 5. Slip velocity along the length of h=5 μm.

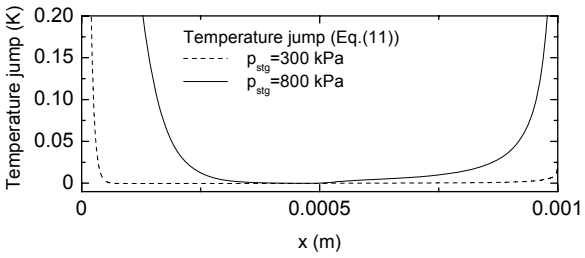

Fig. 6. Temperature jump on the wall of h=5 μm.

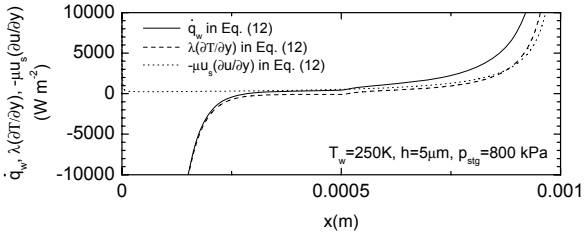

(a) Heated case

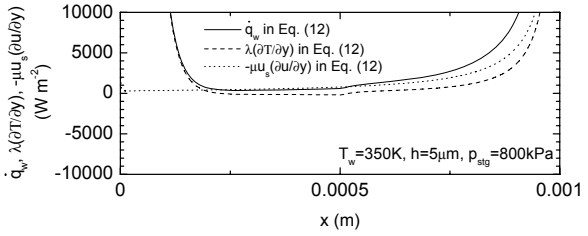

(b) Cooled case

Fig. 7. Heat flux from the wall of h=5 μm.

3.3 Estimation of total temperature

Attention will now be turned to be the bulk temperature of the fluid, T_b, and it is defined as

$$T_b = \int \rho C_p \, u T \, dA \Big/ \int \rho C_p \, u \, dA \tag{17}$$

The bulk temperature of an incompressible laminar flow in a duct is expressed as a function of a mean Nusselt number and the location as (e.g. Burmeister [31])

$$T_b = T_w - (T_w - T_{in})\, e^{-4Nu_m X^*} \tag{18}$$

where Nu_m is the mean Nusselt number of a simultaneously developing flow in a duct and X^* is the inverse of Graetz number defined by

$$X^* = \frac{x}{D_h \, Re \, Pr} \tag{19}$$

Note that the Nu_m is also the function of X^*. The laminar heat transfer characteristics for duct flows have been investigated by many researchers and Nusselt numbers were reported in literatures (e.g. Shah et al. [32]). The numerically obtained Nu_m for the simultaneously developing flow of Pr=0.72 in the channel by Hwang and cited in Shah et al. [32] was used for the calculation of the static bulk temperature for the incompressible flow. The calculated bulk temperatures for a channel are listed in our previous report, (Asako et al. [20]).

The values of $(T_b - T_{stg})/(T_w - T_{stg})$ of T_w = 350 and 250 K are plotted as the function of X^* in Figs. 8(a) and (b), with the

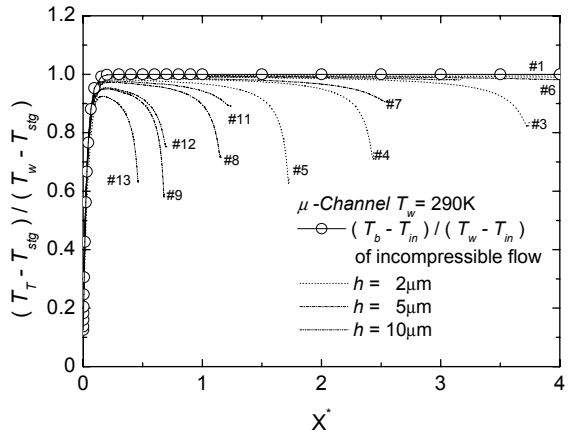

(a) T_w=290 K

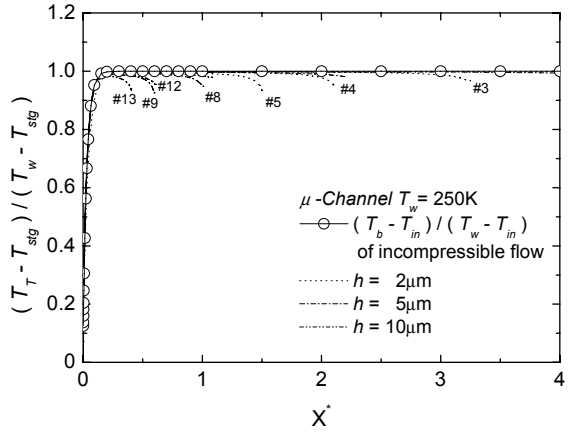

(b) T_w=250 K

Fig. 10. Total temperature as a function of X^* for cooled cases.

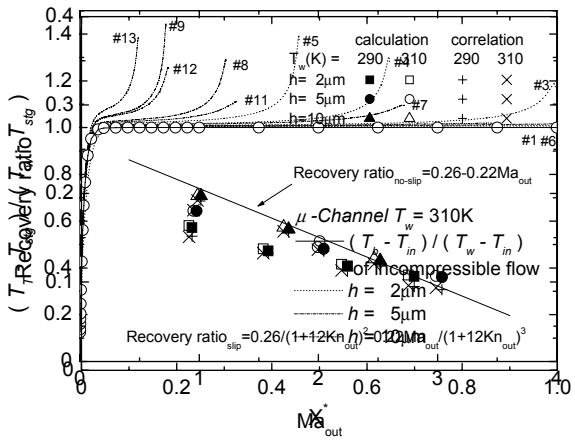

(a) T_w=310K and T_w=290 K

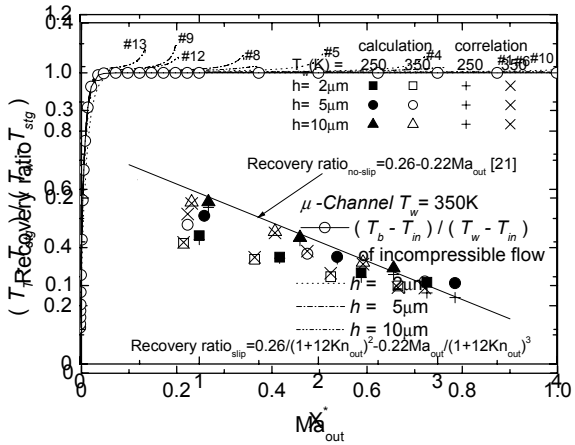

(b) T_w=350K and T_w=250 K

Fig. 9. Total temperature as a function of X^* for heated cases.
Fig. 11. Recovery ratio as function of Ma_{out}.

bulk temperature for the incompressible flow (Eq. (18)), respectively. The value of the bulk temperature for the incompressible flow is normalized as $(T_b - T_{in})/(T_w - T_{in})$. As seen in Fig. 8(a), in the heated case, the normalized bulk temperature of the gaseous flow increases along the channel to the downstream, and levels off and it decreases approaching to the outlet due to the conversion of the thermal energy into the kinetic energy. On the other hand, in the cooled cases (Fig. 8(b)), it also increases along the channel to the downstream, however, it takes a value over unity, approaching to the outlet due to the conversion of the thermal energy into the kinetic energy. The qualitatively same tendency can be seen for each heated case (T_w =310 K) and cooled case (T_w =290 K). As a result, in case of the slow flow (Ma_{out} < 0.3), the normalized bulk temperature almost coincides with that of incompressible flow and does not depend on the wall temperature. However, in case of the fast flow (Ma_{out} > 0.3), the normalized bulk temperature takes a value greater than unity when the wall temperature is lower than the inlet temperature. However, the normalized bulk temperature takes a value less than unity when the wall temperature is higher than the inlet temperature. Therefore the normalized bulk temperature takes a different value depending on whether the wall temperature is higher or lower than inlet temperature.

Attention will now be turned to the total temperature of the fluid, T_T, and it is defined as

$$T_T = \frac{\int \rho C_p u T dA + \int \rho u \frac{u^2}{2} dA}{\int \rho C_p u dA}. \quad (20)$$

The values of $(T_T - T_{stg})/(T_w - T_{stg})$ for both heated and cooled cases are plotted as a function of X^* in Figs. 9 and 10 with the bulk temperature for the incompressible flow, respectively. The value of the bulk temperature for the incompressible flow is normalized as $(T_b - T_{in})/(T_w - T_{in})$. As can be seen in Figs. 9(a) and (b), in the heated cases, the values of $(T_T - T_{stg})/(T_w - T_{stg})$ increase when the total temperature increases because $T_w - T_{stg}$ takes the positive value. On the other hand, in the cooled cases (Figs. 10(a) and (b)), the values of $(T_T - T_{stg})/(T_w - T_{stg})$ decrease when the total temperature increases because $T_w - T_{stg}$ takes the negative value. The total temperature of is slightly lower or higher than the bulk

temperature of the incompressible flow when the flow is slow. However a part of the thermal energy converts into the kinetic energy near the outlet when the flow is fast. This results in the temperature fall and the additional heat transfer is occurred near the outlet as shown in Figs. 2 and 3. Namely, the additional heat transfer due to the temperature fall corresponds to the increment of the total temperature. The maximum increment of the total temperature is less than 10% of $T_w - T_{stg}$ in the cases of T_w = 250 and 350 K (Fig. 9(b) and Fig. 10(b)). However, in the case of T_w = 290 and 310 K (Fig. 9(a) and Fig. 10(a)), the maximum increment reaches 40% of $T_w - T_{stg}$. Namely, in the case of large temperature difference, the additional heat transfer due to the temperature fall is not much. This fact indicates that the heat transfer of the gaseous flow in the micro-channel can be predicted from correlation for the incompressible flow in a conventional sized channel, if the temperature difference $T_w - T_{stg}$ is greater than 50 K. However, if the temperature difference $T_w - T_{stg}$ is less than 50 K, the additional heat transfer becomes relatively large and the heat transfer for the gaseous flow in the micro-channel can not be predicted from correlation for the incompressible flow in a conventional sized channel.

The gas temperature decreases near the outlet due to the energy conversion into the kinetic energy for both heated cases and cooled cases as shown in Figs. 2 and 3. If the thermal conductivity of the gas is extremely high, the gas temperature at the outlet recovers to the wall temperature. However, in actual situation, a slight recovery is observed. Then, the ratio of the actual recovery and the dynamic temperature is defined as

$$\text{Recovery ratio} = \frac{T_T - T_{b,incomp}}{\int \rho u \frac{u^2}{2} dA \Big/ \int \rho C_p u dA} \quad (21)$$

where the denominator represents the dynamic temperature, T_k. Note that the temperature difference between the total temperature and the bulk temperature of the incompressible flow represents the recovery temperature. The recovery ratio calculated from Eq. (21) for all cases is plotted in Fig. 11 as the function of the Mach number at the outlet. For the case of slow flow, the temperature difference between the total temperature and the bulk temperature of the incompressible flow and the dynamic temperature are very low, therefore, they are not plotted in the figure. The ratio is independent of the wall temperature and decreases with increasing the Mach number at the outlet. Eq. (21) can be rewritten as

$$T_T = T_{b,incomp} + \text{Recovery ratio} \times \frac{\int \rho u \frac{u^2}{2} dA}{\int \rho C_p u dA}. \quad (22)$$

Then, the total temperature of the gaseous flow in a micro-channel can be predicted from the bulk temperature of the incompressible flow, the recovery ratio and the dynamic temperature for both heated and cooled cases. The solid line in Fig. 11 represents the correlation for the recovery ratio and Mach number at the outlet in no-slip flow regime (Hong and Asako [22]). In slip flow regime, the correlation for the recovery ratio, outlet Mach number and outlet Knudsen number is obtained as:

$$\text{Recovery ratio} = \frac{0.26}{(1+12Kn_{out})^2} - \frac{0.22Ma_{out}}{(1+12Kn_{out})^3}. \quad (23)$$

The dashed line and the dotted line represent recovery ratio in the case of Kn=0.01 and Kn=0.02 of Eq. (23), respectively. The recovery ratio of slip flow regime is lower than that of no-slip regime since the rarefaction effect due to reduction on the hydraulic diameter is more significant than compressibility effect. However, in the case of Ma_{out}>0.6, it almost coincides with that of no-slip flow regime since the compressibility effect is more dominant than the rarefaction effect.

4. Concluding remarks

Two-dimensional compressible momentum and energy equations with slip boundary conditions have been solved to obtain the heat transfer characteristics of gaseous slip flow in a micro-channel with constant wall temperature, whose temperature is higher or lower than the inlet temperature. The following conclusions were obtained:

(1) Heat transfer characteristics of the gaseous (compressible) flow are different from those of the liquid (incompressible) flow. And they are also different from each cooled and heated case.

(2) The following correlation for the prediction of the heat transfer rate of gaseous flow in a micro-channel is independent of the wall temperature. Also the total temperature of the gaseous flow can be predicted from the bulk temperature of the incompressible flow, the recovery ratio, and the dynamic temperature for both heated and cooled case & both no-slip and slip flow regime.

$$\text{Recovery ratio} = \frac{0.26}{(1+12Kn_{out})^2} - \frac{0.22Ma_{out}}{(1+12Kn_{out})^3}.$$

Nomenclature

A : Per-cycle transfer area per unit depth, m
C_p : Specific heat, J/(kgK)
D_h : Hydraulic diameter(=2h) , m
f : Friction factor, -
F : Maxwell's reflection coefficient, -
h : Channel height, m
i : Specific internal energy, J/(kg)
Kn : Knudsen number, -
ℓ : Channel length, m

$\dot{m}$: Total mass flow rate per unit depth, kg/(m·s)
Ma : Mach number, Eq. (15)
Nu_m : Mean Nusselt number, -
p : Pressure, Pa
Pr : Prandtl number, -
$\dot{q}$: Heat flux, W/m^2
R : Gas constant, J/(kg·K)
Re Reynolds number, Eq. (15)
T : Temperature, K
T_b : Bulk temperature, K
$T_{b,incomp}$: Bulk temperature of incompressible flow, K
T_k : Dynamic temperature, K
T_T : Total temperature, K
T_w : Wall temperature, K
u, v : Velocity components, m/s
x, y : Coordinates, m
X^* : Dimensionless axial length, Eq. (19)
γ : Specific heat ratio, -
λ : Thermal conductivity, W/(m·K)
μ : Viscosity, Pa·s
ρ : Density, kg/m^3
σ : Molecular mean free path, m

subscript

in : Inlet
out : Outlet
s : Slip flow
stg : Stagnation value

References

[1] P. Wu and W. A. Little, Measurement of the heat transfer characteristics of gas flow in fine channel heat exchangers used for microminiature refrigerators, *Cryogenics* 24 (1984) 415-420.

[2] S-H. Ryi, J-S. Park, S-H. Choi, S-H. Cho and S-H. Kim, Novel micro fuel processor for PEMFCs with heat generation by catalytic combustion, *Chemical Engineering Journal*, 113 (2005) 47-53.

[3] R. K. Prud'homme, T. W. Chapman and J. R. Bowen, Laminar compressible flow in a tube, *Appl. Sci. Res*. 43 (1986) 67-74.

[4] H. Sun and M. Faghri, Effect of rarefaction and compressibility of gaseous flow in micro channel using DSMC, *Numerical Heat Transfer, Part A* 38 (2000) 153-158.

[5] T. Araki, M. S. Kim, K. Inaoka and K. Suzuki, An experimental investigation of gaseous flow characteristics in microchannels, *Microscale Thermophysical Engineering* 6 (2002) 117-130.

[6] Y. Asako, T. Pi, S. E. Turner and M. Faghri, Effect of compressibility on gaseous flows in micro-channels, *International Journal of Heat and Mass Transfer* 46 (2003) 3041-3050.

[7] Y. Asako, K. Nakayama and T. Shinozuka, Effect of compressibility on gaseous flows in micro-tube, *International Journal of Heat and Mass Transfer* 48 (2005) 4985-4994.

[8] E. B. Arkilic, M. A. Schmidt and K. S. Breuer, Gaseous flow in microchannel, *ASME Symposium on Micro Machining and Fluid Mechanics* (1994) 1-10.

[9] A. Beskok and G. E. Karniadakis, Simulation of heat and momentum transfer in complex microgeometries, *Journal of Thermomphysics Heat Transfer* 8 (4) (1994) 647-655.

[10] A. Beskok, G. E. Karniadakis and W. Trimmer, Rarefaction and compressibility effects in gas microflows, *Journal of Fluid Engineering* 118 (1996) 448-456.

[11] I. Ahmed and A. Beskok, Rarefaction, compressibility, and viscous heating in gas microfilter, *Journal of Thermophysics and Heat Transfer* 16 (2) (2002) 161-170.

[12] M. Renksizbulut, H. Niazmand and G. Teracan, Slip-flow and heat transfer in rectangular microchannels with constant wall temperature, *International Journal of Thermal Sciences*, 45 (2006) 870-881.

[13] S. E. Turner, L. C. Lam, M. Faghri and O. J. Gregory, Experimental investigation of gas flow in microchannel, *Journal of Heat Transfer* 127 (2004) 753-763.

[14] C. Hong, Y. Asako, S. E. Turner and M. Faghri, Friction factor correlations for gas flow in slip flow regime, *Journal of Fluids Engineering* 129 (2007) 1268-1276.

[15] C. Hong, Y. Asako and M. Faghri, Friction factor correlations of slip flow in micro-tubes, *Proc. 5th Int. Conference on Nanochannels, Microchannels and Minichannels*, Puebla, Mexico, ICNMM2007-30064 (2007).

[16] C. Hong, Y. Asako and J-H. Lee, Poiseuille number correlation for high speed micro-flows, *J. Phys. D: Appl, Phys.* 41 (2008) 105111 (10pp).

[17] N. G. Hadjiconstantinou and O. Simek, Constant-wall temperature nusselt number in micro and nano-channels, *Journal of Heat Transfer* 124 (2002) 356-364.

[18] O. Aydin and M. Avci, Heat and fluid flow characteristics of gases in micropipes, *International Journal of Heat and Mass Transfer*, 49 (2006) 1723-1730.

[19] S. E. Turner, Y. Asako and M. Faghri, Convection heat transfer in microchannels with high speed gas flow, *Journal of Heat Transfer*, 129 (2007) 319-328.

[20] Y. Asako and H. Toriyama, Heat transfer characteristics of

gaseous flows in micro-channels, *Microscale Thermophysical Engineering* 9 (2005) 15-31.
[21] C. Hong, Y. Asako and J-H. Lee, Heat transfer characteristics of gaseous flows in microchannels with constant heat flux, *International Journal of Thermal Sciences* 46 (2007) 1153-1162.
[22] C. Hong and Y. Asako, Heat transfer characteristics of gaseous flows in a microchannel and a micortube with constant wall temperature, *Numerical Heat Transfer, Part A* 52 (2008) 219-238.
[23] C. Hong and Y. Asako, Heat transfer characteristics of gaseous flows in microtube with constant heat flux, *Applied Thermal Engineering* 28 (2008) 1375-1385.
[24] C. Hong and Y. Asako, Heat transfer characteristics of gaseous flows in microchannels with negative heat flux, *Heat Transfer Engineering* 29 (9) (2008) 805-815.
[25] S. G. Kandlikar and W. J. Grande, Evolution micro-channel flow passages-thermohydraulic performance and fabrication technology, *Heat Transfer Engineering* 24 (1) (2003) 3-17.
[26] G. Karniadakis and A. Beskok, Micro flows, fundamentals and simulation, *Springer* (2002).
[27] E. M Sparrow and S. H. Lin, Laminar heat transfer in tubes under slip-flow conditions, *Journal of Heat Transfer*, 84 (1962) 363-369
[28] C. Hong and Y. Asako, Some considerations on thermal boundary condition of slip flow, *International Journal of Heat and Mass Transfer* 53 (2010) 3075-3079.
[29] K. C. Karki, A calculation procedure for viscous flows at all speeds in complex geometries, *Ph. D. thesis, University of Minnesota* (1986).
[30] A. A. Amsden, H. M. Ruppel and C. W. Hire, SALE a simplified ALE computer program for fluid flow at all speeds, *Los Alamos Scientific Lab Report* LA-8095 (1980).
[31] L. C. Burmister, Convective heat transfer, *Wiley*, New York, (1983).
[32] R. K. Shah and A. L. London, Laminar flow forced convection in ducts, advances in heat transfer supplement 1, *Academic Press*, New York (1978).

Chungpyo Hong received his Ph.D. in mechanical engineering from Tokyo Metropolitan University in 2007. His current research area is the fluid flow and heat transfer of gaseous flows in microchannels and gas-micro-heat exchanger. He is currently an assistant professor of the Department of Mechanical Engineering at Tokyo University of Science, Chiba, Japan.